An Improved Rational Model with Memory for the Digital Baseband Predistortion of Power Amplifiers

Victor Gerson Matoso Francisco and Eduardo Gonçalves de Lima

***Abstract*—The use of models described by the ratio of two polynomial approximations with memory has been receiving particular attention by the wireless communication community. Rational models with memory require a lower number of coefficients and work better with extrapolation data than polynomial approximations. This work proposes a novel rational model with memory that, in comparison with previous approaches having the same number of parameters, can increase the modeling accuracy. The novelties of the proposed rational model, in comparison with the best available rational model, are the use of a larger set of truncation factors and the inclusion of additional terms.**

Keywords—Modeling, power amplifier, predistortion, radio frequency, rational model, wireless communication systems.

I. INTRODUCTION

Linearity is a fundamental requirement for modern wireless communication systems [1]. Indeed, the transmission of an enormous amount of information, at tremendously large data rates, through the available bandwidth, is achieved by the use of a radio frequency (RF) carrier modulated by a complex-valued envelope (having variable amplitude and phase components) in which the peak to average amplitude ratio is very high [1]. Linearity is mandatory in order to avoid interferences among users allocated at adjacent channels.

In modern wireless communication systems, the improvement of power efficiency is highly desirable [2]. From what concerns portable devices, the main objective is to extend the time interval between two consecutive battery recharges. From what concerns base stations, the motivation is economical, in particular to reduce the costs associated with energy consumption and heat dissipation [2].

In a wireless communication system, the device that consumes the large amount of energy is the power amplifier (PA) present at the transmitter chain [3]. However, to comply with the linearity specifications imposed by regulatory agencies, the PA efficiency is very poor. In fact, the PA trades off linearity and power efficiency. In one hand, the PA has low efficiency when driven at small signal linear regimes. On the other hand, the PA highest efficiency is observed at large signal nonlinear regimes [3].

To simultaneously achieve high power efficiency and high linearity, an option is to include a digital baseband predistortion (DPD) in the wireless transmitter [4]. In this case, the PA is allowed to operate at its maximum efficiency and the DPD block is responsible for compensating for the nonlinearities introduced by the PA.

For the proper operation of the DPD scheme, additional hardware that will also consume energy is necessary. Hence, when designing a DPD scheme, it is very important to keep at reduced levels the power consumption of the additional hardware. In fact, the overall wireless transmitter power efficiency is increased only if the energy consumption of the DPD block is small in comparison with the energy saved inside the PA circuit.

In this scenario, the availability of a model with low computational cost, capable of accurately representing the PA direct and inverse transfer characteristics, plays a major role [5]-[6]. An excellent compromise between computational cost and modeling error is achieved by rational models with memory [7]-[8]. The main advantages of rational models, in comparison with polynomial approximations, are the reduced number of parameters and the improved treatment of extrapolation data.

This work proposes an improved rational model with memory. The novelties of the proposed rational model, in comparison with the rational model of [7], are the use of a larger set of truncation factors and the inclusion of additional terms. Based on data measured on a GaN HEMT class AB PA, the superior performance of the proposed rational model in comparison with the previous rational models of [7] and [8] are reported. In particular, the proposed rational model, in comparison with the previous rational models of [7] and [8] having the same accuracy, requires a reduced number of parameters. Alternatively, the proposed rational model, in comparison with the previous rational models of [7] and [8] having the same number of parameters, improves the modeling accuracy.

This work is organized as follows. Section II describes the basic concepts of DPD. Section III first reviews the previous rational models and then introduces the proposed rational model. Section IV assesses the accuracies of the different rational models with memory. Section V summarizes the conclusions.

II. DIGITAL BASEBAND PREDISTORTION OF PAS

In an RF PA energy from dc sources is converted into RF output power. Ideally, the RF output signal must be an amplified and linear replica of the RF signal applied at the PA input. However, to improve the efficiency, PAs must be driven at strong gain compression regimes, where significant nonlinear behaviors are observed. As a consequence, when a band-limited signal is processed through a nonlinear PA, its bandwidth is widened by the presence of intermodulation distortion (around the fundamental zone, e.g. around the carrier

Victor Gerson Matoso Francisco and Eduardo Gonçalves de Lima, Department of Electrical Engineering, Federal University of Paraná, Curitiba-PR, Brazil, E-mails: matosovictor@hotmail.com, elima@eletrica.ufpr.br.

frequency) and harmonic distortion (around harmonic zones, e.g. at integer multiples of the carrier frequency). Output matching networks always present at PA circuits drastically reduce the harmonic distortions. Nevertheless, the intermodulation distortion can not be eliminated by any linear filtering action.

One effective strategy to let the PA be operated at its highest efficiency region, at the same time keeping the intermodulation distortion within mandatory thresholds, is to connect a PA in cascade with a predistorter (PD). Once the power level at the PA input is much lower than the PA output power, in the cascade connection the PA must be placed after the PD. Additionally, the PD must have a transfer characteristic equal to the PA inverse transfer characteristic. In this way, the signals at the input and output of the cascade connection are identical even when the PA exhibits significant nonlinear behaviors. In other words, if the PA and PD transfer characteristics are given by f and $g=f^{-1}$, respectively, then a signal z applied at the input of the cascade connection is still available at the output of the cascade connection because $f(g(z))=f(f^{-1}(z))=z$.

Besides nonlinear behaviors, practical PAs also exhibit dynamic effects, especially because non ideal frequency responses of the bias circuit and input and output matching networks. Therefore, the PA can be seen as a nonlinear system with memory and, as a consequence, the PD operator must also be a nonlinear system with memory.

When designing a PD, a first choice that must be done is between an analog implementation and a digital implementation. Digital PDs (DPDs) are preferable than analog PDs because available digital hardwares (for example, digital signal processors and field programmable gate arrays) can construct arbitrarily nonlinear operators with high fidelity and reduced cost.

In a non recursive discrete-time nonlinear model with memory, the instantaneous sample of the DPD output signal must be formulated as a nonlinear function of the instantaneous and previous (up to the memory depth M) samples of the DPD input signal. Moreover, the time interval between two consecutive samples must comply with the Nyquist criterion, which states that continuous-time signals must be sampled at rates larger than twice the highest signal frequency.

In wireless communication systems, the PA real-valued RF input signal, $x(n)$, is a carrier signal at frequency ω_c (on the GHz range) modulated by a complex-valued envelope signal, $\tilde{x}(n)$, having bandwidth on the order of several MHz, according to

$$x(n) = \mathrm{Re}\left[\tilde{x}(n)\, e^{j\omega_c n}\right] = a_x(n)\cos\left[\omega_c n + \theta_x(n)\right]. \quad (1)$$

A DPD able to compensate for all the PA nonlinear dynamic behaviors (both intermodulation and harmonic distortions) must deal with the real-valued RF signals. To comply with the Nyquist criterion, such RF DPD must be sampled at extremely high rates, in particular with sampling frequencies set on several harmonics of the carrier frequency ω_c. However, as previously point out, the harmonic distortions at the PA output can be reduced to negligible levels by a proper design of the output matching networks and, therefore, the PA real-valued RF output signal, $y(n)$, is also a carrier signal at frequency ω_c (on the GHz range) modulated by a complex-valued envelope signal, $\tilde{y}(n)$, according to

$$y(n) \approx \mathrm{Re}\left[\tilde{y}(n)\, e^{j\omega_c n}\right] = a_y(n)\cos\left[\omega_c n + \theta_y(n)\right]. \quad (2)$$

In (2) the approximation symbol is employed to emphasize that the harmonic distortions were neglected. It is worth mentioning that the bandwidth of $\tilde{y}(n)$ is larger than the bandwidth of $\tilde{x}(n)$ due to the intermodulation distortions introduced by the PA. However, $y(n)$ is still a bandpass signal in which the center frequency (ω_c) is much higher than the bandwidth of $\tilde{y}(n)$.

Therefore, a DPD able to compensate only for the intermodulation distortions produced by the PA can provide the necessary level of linearization. Furthermore, the bandpass nature of the PA input and output signals can be exploited in order to achieve a DPD with high accuracy and low computational cost. Indeed, a substantial reduction in the sampling frequency of a DPD is possible if the DPD deals just with the complex-valued envelope signals $\tilde{x}(n)$ and $\tilde{y}(n)$. In fact, in these baseband DPDs, able to compensate only for the intermodulation distortions produced by the PA, the DPD operator g estimates the instantaneous sample of the complex-valued output envelope as a function of the instantaneous and previous samples of the complex-valued input envelope, in this way keeping no connection with the carrier frequency and, therefore, its sampling frequency can be set on the order of the envelope bandwidths.

A baseband DPD can only compensate for distortions at the fundamental zone (in the vicinity of $1\omega_c$). Nevertheless, baseband DPD operators do not retain any connection with ω_c. As a consequence, baseband DPD operators can easily generate contributions at harmonic frequencies of ω_c that for sure will not contribute for the compensation of intermodulation distortions introduced by the PA. This statement is in accordance with the following example. Given the complex-valued envelope $\tilde{x}(n)$, observe that its polar angle component $\theta_x(n)$ is intrinsically connected to ω_c by the relationship $1[\omega_c n + \theta_x(n)]$. If the baseband DPD performs the operation $\tilde{x}^2(n)$, then a contribution at the second harmonic zone ($2\omega_c$) is generated that, certainly, can not compensate for any PA distortion at the fundamental zone ($1\omega_c$). In fact, $\tilde{x}^2(n)$ is equivalent to $a_x^2(n)\exp[j(2\theta_x(n))]$ and, by the connection between $\theta_x(n)$ and ω_c, $2[\omega_c n + \theta_x(n)]$ is obtained, which clearly is a contribution at the second harmonic zone ($2\omega_c$). Therefore, attention must be paid in order to select a baseband DPD operator g that manipulates the polar angle component of complex-valued envelopes in a way that the unitary scalar value multiplying the carrier frequency ω_c is preserved.

In practice, the operator g of a baseband DPD is implemented by a mathematical nonlinear model with memory, having adjustable coefficients to be obtained based on terminal input-output measurements performed at the PA. Indeed, for obtaining the coefficients of the operator g (e.g. an operator having the PA inverse transfer characteristic), it is necessary to exchange the roles of the PA input and output signals. Specifically, the DPD input signal is the PA output signal and the DPD output signal is the PA input signal.

III. RATIONAL MODELS WITH MEMORY

One class of nonlinear model with memory that has recently attracted the interest by the researchers for the modeling of the PA direct and inverse transfer characteristics is the rational model with memory [7]-[8]. In a rational model with memory, the numerator and denominator are both described by polynomial approximations with memory.

The first use of rational model with memory for the lowpass equivalent behavioral modeling of PAs was reported in [7]. In the model proposed in [7], the instantaneous sample of the complex-valued envelope at the PA output $\tilde{y}(n)$ is dependent on the instantaneous and past samples of the complex-valued envelope at the PA input $\tilde{x}(n-m)$ according to

$$\tilde{y}(n)=\frac{\sum_{p=1}^{P_1}\sum_{m=0}^{M_1}\tilde{b}_{p,m}\tilde{x}(n-m)\left[a_x(n-m)\right]^{p-1}}{1+\sum_{p=1}^{P_2}\sum_{m=0}^{M_2}\tilde{e}_{p,m}\left[a_x(n-m)\right]^{p}}, \quad (3)$$

where P_1 and P_2 are polynomial order truncations, M_1 and M_2 are memory lengths, $\tilde{b}_{p,m}$ and $\tilde{e}_{p,m}$ are complex-valued parameters. It is worth mentioning that (3) can also be applied to implement a baseband DPD operator, by just exchanging the input and output roles.

In (3), the unitary scalar value multiplying the carrier frequency ω_c is always preserved. Therefore, as discussed in Section II, (3) only generates contributions at the fundamental zone ($1\omega_c$). In this way, when applied as a baseband DPD, all the contributions provided by (3) do contribute to compensate for the PA intermodulation distortions. The proof is as follows. First, observe that each complex-valued input envelope $\tilde{x}=a_x\exp(j\theta_x)$, independent of the particular time instant, is related to the real-valued RF signal x by $a_x(n)\cos\{1[\omega_C n+\theta_x(n)]\}$ and so, represents a contribution located at the vicinity of ($1\omega_c$). Second, observe that each real-valued amplitude (a_x) component of the input envelope, independent of the particular time instant, is indeed a contribution located at the vicinity of ($0\omega_c$), because $a_x=a_x\exp[j0(\theta_x)]$, which is related to the real-valued RF signal x by $a_x(n)\cos\{0[\omega_C n+\theta_x(n)]\}$. Third, observe that when the product among input amplitude informations is performed, the result is still a contribution located at the vicinity of ($0\omega_c$). For example, $a_x^3=a_x^3\exp[j(0+0+0)(\theta_x)]$, which is related to the real-valued RF signal x by $a_x^3(n)\cos\{0[\omega_C n+\theta_x(n)]\}$. At this moment, it is immediate to see that the denominator of (3) only provides baseband contributions (around $0\omega_c$). Fourth, observe that the product between a baseband contribution and a contribution at the fundamental zone is a contribution around ($1\ \omega_c$). For instance, $\tilde{x}a_x^4=a_x^5\exp[j(1+0+0+0+0)(\theta_x)]$. Therefore, the numerator of (3) only provides contributions around $1\omega_c$. Finally, observe that the division between a contribution at the fundamental zone, provided by the numerator of (3), and a baseband contribution, provided by the denominator of (3), is again a contribution around ($1\omega_c$), which concludes the proof. For example $\tilde{x}a_x^2/a_x^1=a_x^{3-1}\exp[j(1+0+0-0)(\theta_x)]$.

Recently, in [8] a modified rational model was proposed. In particular, the model proposed in [8] is described by the following constitutive equation

$$\tilde{y}(n)=\frac{\sum_{p=1}^{P_1}\sum_{m=0}^{M_1}\tilde{b}_{p,m}\tilde{x}(n-m)\left[a_x(n-m)\right]^{p-1}}{1+\sum_{p=0}^{P_2}\tilde{e}_{p,0}\tilde{x}(n)\left[a_x(n)\right]^{p}}, \quad (4)$$

where P_1 and P_2 are polynomial order truncations, M_1 is a memory length, $\tilde{b}_{p,m}$ and $\tilde{e}_{p,0}$ are complex-valued parameters. There are mainly two differences between (3) and (4), both of them at the denominators. First, the denominator of (4) uses the input envelope only at the present time instant n. Second, while the denominator of (3) requires just the input amplitude component a_x, the denominator of (4) also employs the complex-valued input envelope $\tilde{x}$. Based on the previous proof, it is immediate to see that the model of (4) does not guarantee that only contributions at the fundamental zone ($1\omega_c$) are generated.

In this work, a novel rational model is proposed. In the proposed model, the instantaneous sample of the complex-valued envelope at the PA output is obtained using

$$\tilde{y}(n)=\frac{\tilde{y}_{NUM}(n)}{1+\sum_{p=1}^{P_4}\tilde{e}_{p,0}\left[a_x(n)\right]^{p}+\sum_{p=1}^{P_5}\sum_{m=1}^{M_5}\tilde{h}_{p,m}\left[a_x(n-m)\right]^{p}}, \quad (5)$$

where P_4 and P_5 are polynomial order truncations, M_5 is a memory length, $\tilde{e}_{p,0}$ and $\tilde{h}_{p,m}$ are complex-valued parameters and $\tilde{y}_{NUM}(n)$ is given by

$$\begin{aligned}\tilde{y}_{NUM}(n)=&\sum_{p=1}^{P_1}\tilde{b}_{p,0}\tilde{x}(n)\left[a_x(n)\right]^{p-1}+\\&+\sum_{p=1}^{P_2}\sum_{m=1}^{M_2}\tilde{c}_{p,m}\tilde{x}(n-m)\left[a_x(n-m)\right]^{p-1}+\\&+\sum_{p=2}^{P_3}\sum_{m=1}^{M_3}\tilde{d}_{p,m}\tilde{x}(n)\left[a_x(n-m)\right]^{p-1},\end{aligned} \quad (6)$$

where P_1, P_2 and P_3 are polynomial order truncations, M_2 and M_3 are memory lengths, $\tilde{b}_{p,0}$, $\tilde{c}_{p,m}$ and $\tilde{d}_{p,m}$ are complex-valued parameters.

Observe that the proposed rational model given by (5), as was the case with the previous rational model of (3), only generates contributions at the fundamental zone ($1\omega_c$). Indeed, the numerator of (5) provides just contributions around $1\omega_c$ and the denominator of (5) provides only contributions around $0\omega_c$.

The main advantages of the proposed rational model of (5) in comparison with the previous rational model of (3) are twofold. First, the proposed rational model of (5) includes additional terms not available at the rational model of (3). Second, the proposed rational model of (5) has a larger set of truncation factors in comparison with the previous rational model of (3). In fact, (5) has 8 truncation factors (P_1, P_2, P_3, P_4,

P_5, M_2, M_3 and M_5), while (3) has only 4 truncation factors (P_1, P_2, M_1 and M_2). Therefore, in a comparison between (3) and (5), in a scenario of same number of parameters, it is expected that the proposed rational model provides a better accuracy due to the aforementioned advantages.

IV. EXPERIMENTAL VALIDATION

In this section, the accuracies of the rational models with memory discussed in Section III are comparatively assessed. From now on, the rational model introduced in [7] and described by (3) is designated by "previous 1", the rational model introduced in [8] and described by (4) is designated by "previous 2", and the rational model proposed in this work and described by (5) is designated "proposed".

The three rational models are applied to model the direct and inverse transfer characteristics of a GaN HEMT class AB PA. The complex-valued envelopes at the PA input and output were measured by a Rohde & Schwarz FSQ vector signal analyzer (VSA) at a sampling frequency of 61.44 MHz. The PA was excited by a carrier at 900 MHz modulated by a 3GPP WCDMA signal having a bandwidth of 3.84 MHz. The PA average output power was set to 26 dBm. A total of 33780 samples were captured. Exactly 24180 samples are used for model identification, while the remaining 9600 samples are used for model validation.

The truncation factors provided by each rational model were varied from their initial values until 5. In particular, the "previous 1" model has 4 truncation factors, namely P_1, P_2, M_1 and M_2, the "previous 2" model has 3 truncation factors, namely P_1, P_2 and M_1, and the "proposed" model has 8 truncation factors, namely P_1, P_2, P_3, P_4, P_5, M_2, M_3 and M_5.

To identify the rational model parameters, the least squares algorithm was applied. For that purpose, each rational model was rewritten in the following way:

$$\tilde{y} = \frac{num[\tilde{x}]}{1+den[\tilde{x}]} \Rightarrow \tilde{y} = num[\tilde{x}] - \tilde{y}den[\tilde{x}]. \qquad (7)$$

To evaluate the rational model accuracies, the normalized mean square error (NMSE), as defined in [9] is calculated according to

$$NMSE = 10\log 10\left[\frac{\sum_{n=1}^{N}\left|out_{DES}(n)-out_{EST}(n)\right|^2}{\sum_{n=1}^{N}\left|out_{DES}(n)\right|^2}\right] \qquad (8)$$

where $out_{DES}(n)$ is the desired output at the time instant n, $out_{EST}(n)$ is the output estimated by the model at the time instant n and N is the total number of sampled input-output data.

A. Modeling of the PA direct transfer characteristic

In this first comparative analysis, the three rational models are applied to the modeling of the PA direct transfer characteristic. Specifically, the rational model input is the complex-valued envelope measured at the PA input and the rational model output is the complex-valued envelope measured at the PA output. Figure 1 shows the best NMSE results for each rational model as a function of the number of parameters. Observe that the "previous 2" model provides much higher errors than the other rational models. In particular, the best NMSE achieved by the "previous 2" model is equal to -36.0 dB. According to Section III, this bad behavior of the "previous 2" model is expected, once it does generate contributions outside the fundamental zone that can not model the intermodulation distortions produced by the PA.

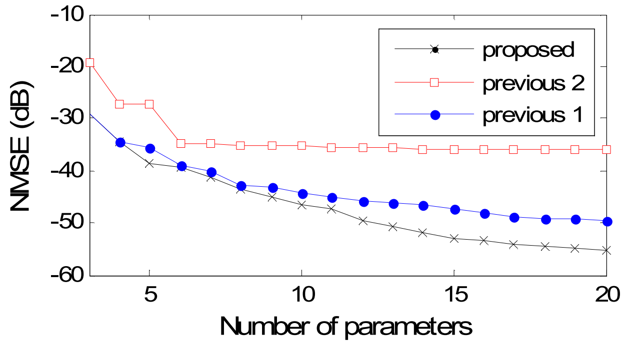

Fig. 1. Best NMSE results as a function of the number of parameters.

From Fig. 1, observe that the "proposed" model, in comparison with the "previous 1" model having the same number of parameters, reduces the NMSE by up to 5.9 dB. Therefore, the use of a larger set of truncation factors and the inclusion of additional terms, provided by the "proposed" model with respect to the "previous 1" model, considerably improve the modeling accuracy.

Figure 2 shows the normalized (measured and simulated by the proposed model) instantaneous output amplitude as a function of the normalized instantaneous input amplitude, the so-called normalized instantaneous AM-AM (amplitude modulation - amplitude modulation) conversion. The direct transfer characteristic estimated by the proposed rational model is in great accordance with the measured characteristic.

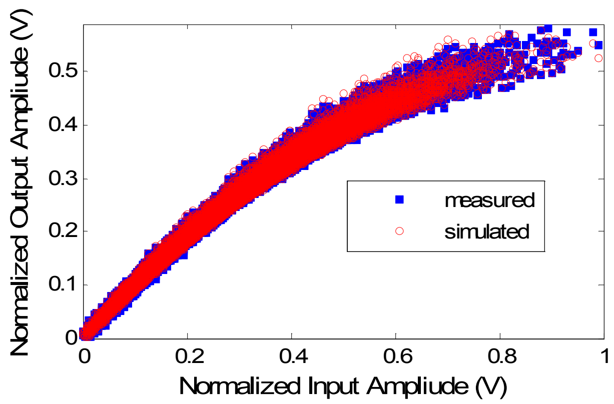

Fig. 2. Normalized instantaneous AM-AM conversions: measured and estimated by the proposed rational model having P_1=2, P_2=1, P_3=1, P_4=1, P_5=2, M_2=2, M_3=1 and M_5=3.

B. Modeling of the PA inverse transfer characteristic

In this second comparative analysis, the three rational models are applied to the modeling of the PA inverse transfer characteristic. Therefore, now the rational model input is the complex-valued envelope measured at the PA output and the rational model output is the complex-valued envelope measured at the PA input. Figure 3 shows the best NMSE results for each rational model as a function of the number of parameters. Once again, the "previous 2" model was not able to provide accuracies as good as the other rational models. The best NMSE achieved by the "previous 2" model is equal to -

32.1 dB, which is 27.5 dB worse than the NMSE achieved by the proposed model. Furthermore, if the “proposed” model is compared to the “previous 1” model having the same number of parameters, improvements in accuracy are clearly noticeable, quantified by reductions in the NMSE metric by up to 9.1 dB. In this way, the advantages of the “proposed” model in comparison with the “previous 1” model are also validated when they are applied to the modeling of the PA inverse transfer characteristic.

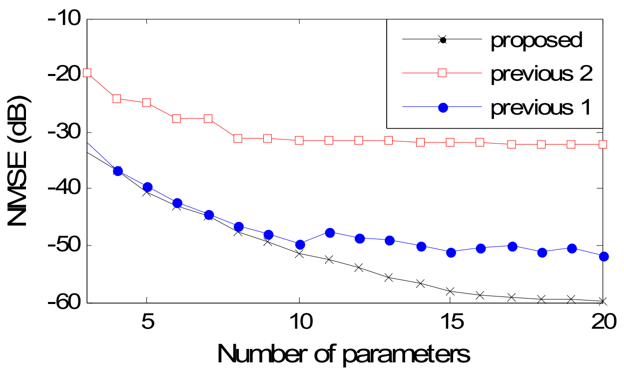

Fig. 3. Best NMSE results as a function of the number of parameters.

V. CONCLUSIONS

This work has presented an improved rational model with memory, suitable for the lowpass equivalent behavioral modeling and digital baseband predistortion of radio frequency power amplifiers present in wireless transmitters. The inclusion of a DPD scheme significantly increases the efficiency of wireless systems. Nevertheless, caution must be taken in order to guarantee that the power consumed by the additional DPD hardware is as low as possible, especially if the DPD is to be included in handsets that handle powers on the order of 1 W.

The proposed rational model with memory, in comparison with previous approaches having the same modeling accuracy, demands for a lower computational complexity and, therefore, can be implemented with a digital hardware that consumes lower power. Specifically, when applied for the modeling of the inverse transfer characteristic of a GaN HEMT class AB PA with an accuracy of -51.3 dB in NMSE, the proposed model requires only 10 complex-valued parameters while the best previous rational model with memory requires 20 complex-valued parameters.

REFERENCES

[1] D. Raychaudhuri, N.B. Mandayam, "Frontiers of Wireless and Mobile Communications," *Proceedings of the IEEE* , vol.100, no.4, pp.824-840, Apr. 2012.

[2] F. H. Raab, P. Asbeck, S. Cripps, P. B. Kenington, Z. B. Popovic, N. Pothecary, J. F. Sevic, and N. O. Sokal, "Power amplifiers and transmitters for RF and microwave," *IEEE Trans. Microw. Theory Tech.*, vol.50, no.3, pp.814–826, Mar. 2002.

[3] S. Cripps, *RF Power Amplifiers for Wireless Communications*, 2nd edition. Norwood, MA: Artech House, 2006.

[4] P. B. Kenington, *High Linearity RF Amplifier Design*. Norwood, MA: Artech House, 2000.

[5] J. C. Pedro and S. A. Maas, “A comparative overview of microwave and wireless power-amplifier behavioral modeling approaches,” *IEEE Trans. Microw. Theory Tech.*, vol. 53, no. 4, pp. 1150–1163, Apr. 2005.

[6] G. Xu, T. Liu, Y. Ye, T. Xu, H. Wen, and X. Zhang, "Generalized Two-Box Cascaded Nonlinear Behavioral Model for Radio Frequency Power Amplifiers With Strong Memory Effects," *IEEE Trans. Microw. Theory Tech.*, vol.62, no.12, pp.2888–2899, Dec. 2014.

[7] T. R. Cunha, P. M. Lavrador, E. G. Lima, and J. C. Pedro, “Rational function-based model with memory for power amplifier behavioral modeling,” in *Proc. Workshop INMMIC*, Apr. 2011, pp. 1–4.

[8] M. Rawat, K. Rawat,F. M. Ghannouchi, S.Bhattacharjee, and H. Leung, “Generalized Rational Functions for Reduced-Complexity Behavioral Modeling and Digital Predistortion of Broadband Wireless Transmitters,” *IEEE Trans. Instrum. Meas.*, vol. 63, no.2, pp.485-498, Feb. 2014.

[9] M. S. Muha, C. J. Clark, A. Moulthrop, and C. P. Silva, “Validation of power amplifier nonlinear block models,” in *IEEE MTT-S Int. Microwave Symp. Dig.*, Anaheim, CA, Jun. 1999, pp. 759–762.